AGU PUBLICATIONS

Geophysical Research Letters

RESEARCH LETTER
10.1002/2017GL074198

Key Points:
- Channel form in steep rivers systematically changes with bed slope for reasons that remain unclear
- Building on previous studies, we identify process variables that control channel form and show how these variables covary with bed slope
- The relationship between channel form and bed slope depends on channel width-to-depth ratio, grain size-to-width ratio, and Froude number

Supporting Information:
- Table S1
- Supporting Information S1

Correspondence to:
M. C. Palucis,
mpalucis@caltech.edu

Citation:
Palucis, M. C., and M. P. Lamb (2017), What controls channel form in steep mountain streams?, *Geophys. Res. Lett.*, *44*, 7245–7255, doi:10.1002/2017GL074198.

Received 17 MAY 2017
Accepted 1 JUL 2017
Accepted article online 6 JUL 2017
Published online 18 JUL 2017

What controls channel form in steep mountain streams?

M. C. Palucis[1] and M. P. Lamb[1]

[1]Division of Geological and Planetary Sciences, California Institute of Technology, Pasadena, California, USA

Abstract Steep mountain streams have channel morphologies that transition from alternate bar to step-pool to cascade with increasing bed slope, which affect stream habitat, flow resistance, and sediment transport. Experimental and theoretical studies suggest that alternate bars form under large channel width-to-depth ratios, step-pools form in near supercritical flow or when channel width is narrow compared to bed grain size, and cascade morphology is related to debris flows. However, the connection between these process variables and bed slope—the apparent dominant variable for natural stream types—is unclear. Combining field data and theory, we find that certain bed slopes have unique channel morphologies because the process variables covary systematically with bed slope. Multiple stable states are predicted for other ranges in bed slope, suggesting that a competition of underlying processes leads to the emergence of the most stable channel form.

1. Introduction

Natural streams rarely have flat beds because mobile bed sediment often forms distinct bed and channel forms, such as ripples, dunes, bars, and alternating steps and pools [e.g., *Rubin and McCulloch*, 1980; *Engelund and Fredsoe*, 1982; *Southard*, 1991]. The presence of these bed morphologies through the channel network is important as they affect hydraulic roughness and flow resistance, which in turn affects flow depth and velocity, sediment transport rates [*Hassan and Reid*, 1990; *Aberle and Smart*, 2003; *Nitsche et al*., 2011; *Lamb et al*., 2017], and bedrock incision rates [e.g., *Johnson and Whipple*, 2010]. Channel state depends on local flow structure, supply of sediment, and forcing/boundary conditions, resulting in feedbacks between hydraulics, sediment transport, and bed topography. Because of the relationship between sediment transport rates and flow resistance, considerable effort has gone into understanding the conditions under which different channel morphologies develop for low gradient sand-bedded streams [e.g., *Vanoni and Hwang*, 1967; *Southard and Boguchwal*, 1990; *Southard*, 1991; *Church and McLean*, 1994; *Venditti*, 2007; *Hendershot et al*., 2016]. Less work, however, has been done for steeper, gravel- and boulder-bedded streams; these channels provide important aquatic habitat [e.g., *Church*, 2002], are conduits for a majority of the sediment delivered to lower gradient channels [e.g., *Milliman and Syvitski*, 1992; *Yager et al*., 2012; *Cui and Parker*, 2005], and comprise much of the channel network in mountainous terrains [*Shreve*, 1969; *Stock and Dietrich*, 2003]. The difficulty in observing active sediment transport events in steep streams, combined with the paucity of data on steep river hydrodynamics has contributed to our lack of understanding of the mechanics behind channel state and stability within steep alluvial channels.

Numerous classifications of channel morphology have been proposed based on field observations [*Rosgen*, 1994, 1996; *Montgomery and Buffington*, 1997; *Wohl and Merritt*, 2008; *Buffington and Montgomery*, 2013], and most of these analyses attribute certain channel forms to distinct ranges in bed slope. For example, *Montgomery and Buffington* [1997] showed that channel state changes from alternate bars to plane bed to steps and pools to cascade morphology (Figure 1) with increasing channel bed slope. Regression analyses have also shown that bed slope, not channel geometry or grain size, is the best predictor of channel type for natural rivers [e.g., *Wohl and Merritt*, 2005; *Flores et al*., 2006; *Altunkaynak and Strom*, 2009]. There is a disconnect, however, between this basic observation that channel morphology depends only on bed slope, and more mechanistic theoretical and experimental investigations into the formation of specific channel states. For example, stability analyses suggest that channel width-to-depth ratios control alternate bar formation [e.g., *Colombini et al*., 1987; *Parker*, 2004], step-pools are hypothesized to result from near Froude critical flow conditions [*Grant et al*., 1990] or channel-width spanning boulders [*Church and Zimmermann*, 2007], and cascade channels are potentially associated with debris flows [*Montgomery et al*., 2003]. If channel state fundamentally depends on variables such as channel width-to-depth ratio, Froude number, and channel width-to-grain size ratio, why then do natural stream morphologies depend most strongly on bed slope?

Figure 1. Alluvial channel-reach morphologies (a) Cascade, Squire Creek, Washington, USA; (b) Step-pool, Fox Creek, California, USA; (c) Plane bed, Rock Creek, California, USA; and (d) Alternate bar, Upper Haukadalsvatn, Iceland. Photo credit: MPL.

Herein, we explore the hypothesis that the controlling process variables for different channel states covary with bed slope in a manner that leads to the systematic correlation between channel morphology and bed slope found in natural streams. We first review current hypotheses for the dominant variables thought to control channel morphology (section 2). Next, we explicitly show how these dominant variables depend on bed slope (section 3), compare the theoretical results to field data (sections 4 and 5), and discuss the implications for predicting unique channel states (section 6).

2. Controlling Variables on Channel Morphology

Alternating bar morphology (Figure 1a) within a stream reach is typically identified by alternating sequences of pools, defined as topographic depressions within the channel, and bar forms, sediment deposits that form topographic highs [*O'Neill and Abrahams*, 1984]. Bar formation in natural channels typically occurs for bed slopes less than $S = 0.03$ [*Montgomery and Buffington*, 1997], where S is the tangent of the bed-slope angle. Flume and field studies have shown that bar and pool topography is generated by lateral flow convergence, where pools are scoured, and regions of flow divergence, where sediment is deposited to form bars [e.g., *Dietrich and Smith*, 1983; *Dietrich and Whiting*, 1989; *Nelson et al.*, 2010]. Theoretical and experimental work suggests that the ratio of the bankfull channel width, B, to bankfull depth, H, strongly influences bar formation, where alternating bars occur at moderately large values ($B/H > 12$) [*Colombini et al.*, 1987, and references within; *Parker*, 2004]. Importantly, despite field observations, alternate bars can be produced in the

laboratory with bed slopes that far exceed $S = 0.03$ [*Bathurst et al*., 1984; *Lisle et al*., 1991; *Weichert et al*., 2008], suggesting that bed slope is not the controlling parameter in their formation.

Stream reaches described as having plane-bed morphology (Figure 1b) lack discrete and/or rhythmic bar forms and have long stretches of relatively featureless beds [*Montgomery and Buffington*, 1997]. The term has been used both for sand-bedded and gravel-bedded channels, though we focus on the latter. Plane bed is often associated with low channel width-to-depth ratios ($B/H < 12$) [e.g., *Colombini et al*., 1987] or larger bed grain diameter (D) to bankfull depth ratios ($0.1 < D/H < 0.8$) [*Montgomery and Buffington*, 1997] as compared to alternate bar reaches.

Step-pool morphologies (Figure 1c) are associated with steeper gradient channels (i.e., $\sim 0.02 < S < \sim 0.2$ [*Abrahams et al*., 1995; *Chin*, 1999; *Zimmermann and Church*, 2001]) and are characterized by a distinctly stepped longitudinal profile. Water flows over and through channel-spanning "steps" composed of large cobbles or boulders before plunging into pools below [e.g., *Chin*, 1989; *Grant et al*., 1990; *Montgomery and Buffington*, 1997], and flow may alternate from Froude critical to supercritical over the steps to subcritical within the pools [*Chin*, 1989]. The mechanisms controlling step formation and stability are most commonly attributed to macroscale antidunes [*Whittaker and Jaeggi*, 1982; *Grant and Mizuyama*, 1991], cyclic steps [*Parker and Izumi*, 2000; *Taki and Parker*, 2005], or a granular jamming mechanism [*Judd*, 1963; *Brayshaw et al*., 1983; *Zimmermann and Church*, 2001; *Zimmermann et al*., 2010]. *Kennedy* [1963] used potential flow theory to derive the theoretical domain over which antidunes can form, which is tied to Froude numbers, $0.7 < Fr < 0.96$ (see supporting information). Cyclic step development is tied to a similar range in Froude numbers at the threshold of motion [*Parker and Izumi*, 2000]. *Church and Zimmermann* [2007] hypothesized that the propensity for jamming is controlled by B/D, termed the jamming ratio. They found that steps formed in both natural and flume channels for jamming ratios $B/D_{84} < 15$ [*Church and Zimmermann*, 2007], where D_{84} is the grain diameter for which 84% of the grains is smaller, and became progressively more stable for $B/D_{84} < 6$ [*Zimmermann et al*., 2010].

Montgomery and Buffington [1997] delineate cascade channels as streams in which energy dissipation is the result of continuous tumbling jet-and-wake flow over large, individual clasts (Figure 1d). These channels typically occur on bed slopes above 0.1, are often confined by valley walls, and are dominated by cobbles and boulders [e.g., *Montgomery and Buffington*, 1997; *Livers and Wohl*, 2015]. Cascade streams are tied to portions of the stream network where debris flows may dominate over fluvial processes ($0.1 < S < 0.7$ [*Stock and Dietrich*, 2003; *DiBiase et al*., 2012]). There has been little work done on the process mechanics that produce cascade morphology. The onset criterion for in-channel debris flows, however, can be framed in terms of a bankfull Shields stress, τ^*_{bf}, relative to a critical Shields stress for bed failure, $\tau^*_{\mathrm{c,df}}$, [*Takahashi*, 1978; *Prancevic et al*., 2014], which we explore further below as a potential discriminator for cascade morphology.

3. Model Development

Here we combine relations from previous work in sediment transport and hydrodynamics to derive expressions that show explicitly the dependence on bed slope for the controlling process variables: Froude number, width-to-depth ratio, jamming ratio, and the ratio of the bankfull Shields stress to the critical Shields stress for in-channel debris flow initiation. In all cases, we chose bankfull flow as our reference condition for formative flows [e.g., *Parker et al*., 1998].

Under the assumptions of normal (i.e., steady and uniform) flow, the Froude number by definition can be written as

$$Fr = \sqrt{\frac{S}{C_f}} \tag{1}$$

where C_f is a frictional resistance coefficient,

$$C_f = \left(\frac{u_*}{\overline{U}}\right)^2, \tag{2}$$

u_* is the bed shear velocity and $\overline{U}$ is the cross sectionally averaged flow velocity [*Garcia*, 2008]. We use the relation of *Ferguson* [2007] for C_f, which has been found to be accurate across a wide range of flow conditions common to mountain streams [*Rickenmann and Recking*, 2011]

$$\frac{\overline{U}}{u^*} = \frac{a_1\left({}^{H}/_{D_{50}}\right)}{\left[\left({}^{H}/_{D_{50}}\right)^{5/3} + \left({}^{a_1}/_{a_2}\right)^2\right]^{1/2}} \tag{3}$$

where $a_1 = 6.5$ and $a_2 = 2.5$ are empirical constants. Equation (3) requires an expression for H/D_{50}, which likely varies with bed slope. Here we utilize a common assumption that coarse-grained rivers evolve to a threshold state such that the bankfull Shields stress does not significantly exceed the critical Shields stress for sediment transport [*Parker*, 1978; *Paola et al*., 1992]. That is

$$\tau^*_{\mathrm{bf}} = r\tau^*_c. \tag{4}$$

The parameter r varies with the Reynold's particle number, Re_p, but is a constant near unity ($1.2 < r < 1.6$) for large Re_p [*Parker*, 1978; *Parker et al*., 2007; *Trampush et al*., 2014], with r closer to 2 in rivers with high sediment supply [*Pfeiffer et al*., 2017]. Under the assumption of normal flow

$$\tau^*_{\mathrm{bf}} = \frac{R_h S}{R D_{50}} \tag{5}$$

where $R = 1.65$ is the submerged specific gravity of the sediment and R_h is the bankfull hydraulic radius. For the critical Shields number, we follow *Lamb et al*. [2008]

$$\tau^*_c = 0.15 S^{0.25}. \tag{6}$$

Combining equations (1)–(6), the Froude number can be expressed as

$$Fr = S^{0.5}\frac{a_1\left(\frac{0.15rR}{S^{0.75}}\right)}{\left[\left(\frac{0.15rR}{S^{0.75}}\right)^{5/3} + \left(\frac{a_1}{a_2}\right)^2\right]^{1/2}} = \frac{1}{S^{0.25}}\frac{a_1 0.15rR}{\left[\left(\frac{0.15rR}{S^{0.75}}\right)^{5/3} + \left(\frac{a_1}{a_2}\right)^2\right]^{1/2}} \tag{7}$$

which is now an explicit function of bed slope and a number of constants.

To express the bankfull width-to-depth ratio (B/H) and jamming ratio (B/D_{84}) as functions of bed slope, we use the semiempirical relations of *Parker et al*. [2007] for bankfull depth, width, and slope,

$$H = \frac{0.382}{g^{1/5}} Q^{2/5} \tag{8}$$

$$B = \frac{4.63}{g^{1/5}} Q^{0.4}\left(\frac{Q}{\sqrt{gD_{50}}D_{50}^2}\right)^{0.0667} \tag{9}$$

$$S = 0.101\left(\frac{Q}{\sqrt{gD_{50}}D^2{}_{50}}\right)^{-0.344} \tag{10}$$

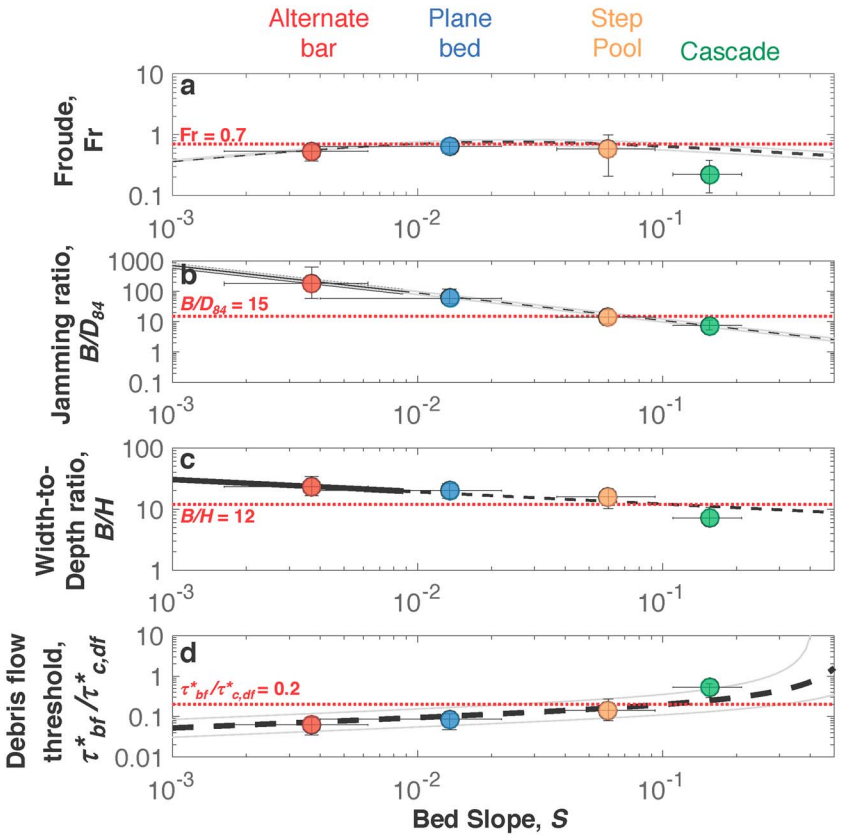

Figure 2. Channel state dimensionless variables as a function of bed slope, *S*. Model results are shown with black lines (where the solid lines denote the slope range of the data from which the *Parker et al.* [2007] relationships were derived), thresholds previously proposed are shown by the red dashed lines, and the median of the field data are plotted for each channel morphology (alternate bar data are colored red, plane bed data are colored blue, step-pool data are colored orange, and cascade data are colored green). Error bars show the central 50% of the data. (a) Froude number (equation (7)) plotted as a function of slope using $a_1 = 6.5$, $a_2 = 2.5$, and r ranging from 1.2 (lower gray line) to 1.6 (upper gray line), with $r = 1.4$ as the best fit to the data; (b) jamming ratio (equation (12)) plotted as a function of slope with r ranging from 1.2 (lower gray line) to 1.6 (upper gray line), with $r = 1.4$ as the best fit to the data with $D_{84}/D_{50} = 2$; (c) width-to-depth ratio (equation (11)) as a function of slope; and (d) ratio of bankfull shear stress to the shear stress needed for debris flow initiation (equation (14)) as a function of slope where $\eta = 0.4$ and the failure plane friction angle (ϕ_o) ranges from 40 (upper gray line) to 60° (lower gray line) [*Selby*, 1993], with the best fit to the data for $\phi_o = 50°$.

where g is gravity, Q is the volumetric bankfull water discharge, and D_{50} is the median diameter of the bed sediment. Combining equations (8)–(10), we find that B/H can be written as a function of bed slope alone

$$\frac{B}{H} = \frac{7.66}{S^{0.2}} \tag{11}$$

To calculate the jamming ratio as a function of S, we combine equations (4)–(6) and (11), and set $\frac{D_{84}}{D_{50}} = 2$ [*Church and Rood*, 1983],

$$\frac{B}{D_{84}} = \frac{2.3Rr}{S^{0.95}}. \tag{12}$$

Finally, to get the ratio of the bankfull Shields stress to the critical Shields stress for in-channel debris flow initiation, we combine equations (4) and (6) with the relation for the critical Shields stress for in-channel debris flow initiation, $\tau^*_{c,df}$, [*Takahashi*, 1978; *Prancevic et al.*, 2014]

$$\tau^*_{c,df} = (1-\eta)(\tan\phi_0 - S) - \frac{S}{R} \tag{13}$$

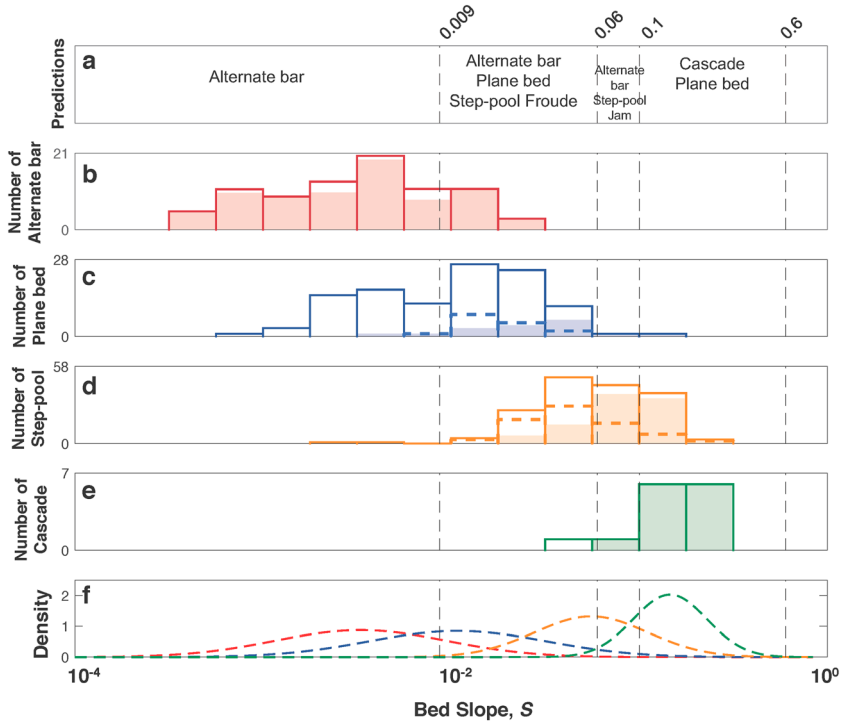

Figure 3. (a) Predictions for the channel morphology as a function of bed slope, where the vertical dashed lines indicate the transition to new channel bed states based on our theory and thresholds shown in Figure 2; (b) histogram of alternate bar data with $\log_{10}$-slope bin widths of 0.25, where the red outlines indicate the total number of alternate bar streams in each bin and the filled region indicates the number of those streams that meet the condition of having a width-to-depth ratio > 12; (c) histogram of the plane bed data with $\log_{10}$-slope bin widths of 0.25, where the solid blue outlines indicate the total number of plane bed streams in each bin, the dashed blue lines indicate the number of those streams that have Froude numbers, Fr, > 0.7 and the filled region indicates those streams with width-to-depth ratios <12; (d) histogram of step-pool data with $\log_{10}$-slope bin widths of 0.25, where the solid orange outlines indicate the total number of step-pool bed streams in each bin, the dashed orange lines indicate the number of those streams with $Fr > 0.7$, and the filled regions indicate those streams with jamming ratios <15; (e) histogram of cascade data with $\log_{10}$-slope bin widths of 0.25, where the solid green outlines indicate the total number of cascade streams in each bin and the filled regions indicate those streams with $\tau^*_{bf}/\tau^*_{c,df} > 0.2$; and (f) normalized probability density functions for each stream type (i.e., the area under the curve is equal to 1).

where η is bed porosity, and ϕ_o is the failure plane friction angle. The resulting expression

$$\frac{\tau^*_{bf}}{\tau^*_{c,df}} = \frac{r0.15S^{0.25}}{(1-\eta)(\tan\phi_0 - S) - \frac{S}{R}} \tag{14}$$

is a function of bed slope and bed material properties (i.e., r, η, and ϕ_o). We assume friction angles in the range of 40° to 60° (typical for natural materials [*Selby*, 1993]) and a porosity of 0.4 (typical of uniform gravel).

4. Data Compilation

To compare our theoretical predictions with field data, we have compiled data from 373 alluvial stream reaches (14 cascade (median r = 2.4), 166 step-pool (median r = 1.2), 110 plane bed (median r = 1.2), and 83 alternate bars (median r = 1.3), where r is calculated from equations (4)–(6)). Many of these reaches were included in previous data compilations [e.g., *Trampush et al.*, 2014; *Li et al.*, 2015], though we have compiled additional data (supporting information Table S1).

5. Results

Equation (7) predicts that Froude number for natural streams steadily increases with bed slope up to S = 0.018, beyond which it decreases (Figure 2a). The maximum Froude number ranges between 0.7 and

0.8, which are the minimum Froude numbers predicted by potential flow theory (lower red line). The data follow the model trend for $r = 1.4$, with the exception of cascade streams, for which the model overpredicts the Froude numbers found in most cascade reaches. The jamming ratio is predicted to decrease with bed slope (power law slope of 0.95; Figure 2b), and equation (12) matches well the median jamming ratio for all stream morphologies. Step formation has been observed in both natural and flume channels for jamming ratios less than or equal to 15 (red dashed line, Figure 2b) [*Church and Zimmermann*, 2007], which coincides with the median jamming ratio for step-pools. In comparison to the jamming ratio, the bankfull width-to-depth ratio (Figure 2c) is predicted to be a weaker function of bed slope ($S^{-0.2}$); the data follow the model trend, with the exception of cascade streams, in which the central 50% of the reported reaches have a lower than expected bankfull width-to-depth ratio. The ratio $\tau^*_{bf}/\tau^*_{c,df}$ increases nonlinearly with bed slope and r (Figure 2d).

Combining the proposed thresholds for the onset of different reach types with model predictions for the bed slopes at which these conditions are expected to be met (Figure 2), we find that certain bed slopes should correlate to unique channel morphologies, whereas other ranges of bed slopes are predicted to have multiple stable channel states (Figure 3a). Channels with $S < 0.009$ are predicted to have alternate bar morphology because steeper slopes tend to have narrower width-to-depth ratios. Indeed, most alternate bar data fall in this range (Figure 3b); however, approximately half of the data for plane bed streams (Figure 3c) also occur at $S < 0.009$. Alternate bars are predicted to occur up to bed slopes as steep as $S = 0.1$ because this range in slopes satisfies the criteria of $B/H > 12$. However, alternate bars are not observed on slopes steeper than 0.025 within our data set.

Step-pool steams are predicted to be stable for $0.009 < S < 0.06$ if they are initiated by the antidune mechanism ("Step-pool Froude," Figure 3a) because both lower and higher channel gradients have too small of Froude numbers. However, this range of slopes is also predicted to support the formation of alternate bars and plane bed morphologies. Indeed, alternate bar (Figure 3b), plane bed (Figure 3c), and step-pool (Figure 3d) data do plot within this slope range. Step-pools that originate via the jamming mechanism are expected to form at $S > 0.06$ (Figure 3a) because this regime correlates with the jamming criteria $B/D_{84} < 15$. Over half of our step-pool data have $0.06 < S < 0.2$ (Figure 3d).

We observe that channels with $\tau^*_{bf}/\tau^*_{c,df} > 0.2$ (Figure 3e) are likely to have a cascade morphology. With this criterion, the majority of the cascade data plot in the regime $S > 0.1$. As plane bed is often assumed to occur at low channel width-to-depth ratios ($B/H < 12$), prior to the onset of alternate bars [e.g., *Colombini et al.*, 1987], we would predict they occur at bed slopes greater than 0.1 (Figure 3a), which is true for only a small subset of the data.

6. Discussion and Conclusion

Our analysis suggests that bed slope is often the best discriminant of the morphological characteristics of steep channel beds because the process variables that control the channel bed state covary with slope for most natural streams (Figure 2). Most of the alternate bar reaches have $S < 0.02$ because these also have bankfull width-to-depth ratios greater than 12. Most step-pool streams have $0.002 < S < 0.2$ because this range in bed slopes correlates either with jamming ratios less than 15, especially those found at slopes greater than 0.06 (as predicted), or Froude numbers greater than 0.7. Cascade reaches tend to have $S > 0.1$ and, for all but one cascade stream (1 out of 14), this correlates with a $\tau^*_{bf}/\tau^*_{c,df} > 0.2$.

Plane bed is a notable exception to the good correlation between controlling variables for a given channel morphology and bed slope. Plane bed streams tend to have low Froude numbers (< 0.7) and width-to-depth ratios greater than 12, which goes against the predictions set from potential flow theory for upper plane bed (i.e., transitional Froude numbers) and linear stability analysis (i.e., low width-to-depth ratios). There is a stable regime for lower (sandy) plane beds characterized by large particle Reynold's numbers (>100) and moderate Shields numbers ($1 < \tau^* < 10$) [*Lamb et al.*, 2012], but we find that in this phase space gravel plane bed data cannot be differentiated from alternate bar and step-pool data.

Setting $r = 2.4$ for channels with high sediment supply [*Pfeiffer et al.*, 2017], the model is generally a poorer predictor of the observed channel state for a given bed slope, which supports our assumption of channels near the threshold for sediment transport at bankfull. Large roughness elements (i.e., immobile boulders),

woody debris, and/or bedrock exposure may also affect r by partitioning stress away from the bed [e.g., *Buffington and Montgomery*, 1999], although it is unclear if drag from large roughness elements systematically changes with bed slope [*Zimmermann*, 2010; *Lamb et al*., 2017].

By combining previous theory with proposed thresholds for channel state emergence and stability, we see that certain bed slopes predict unique channel morphologies, while other slope ranges predict the occurrence of up to three different channel bed types (Figure 3a). The existence of this overlap between predicted channel state and bed slope further suggests that slope is unlikely to be a main control, but rather there are different competing processes and, depending on the local conditions (i.e., confinement, grain size, and sediment supply), this competition may lead to the emergence of different channel morphologies. For example, while alternate bars are predicted to form at fairly steep slopes (bed slopes up to 0.1), channel confinement combined with the influx of large sediment from debris flows or landslides at these steeper slopes might result in more favorable conditions for step-pool formation. In fact, within the field data, we observe an abrupt handoff between alternate bar and step-pools around slopes of ~0.02 to 0.03, which is the lower bound for debris flow deposition based on case studies in the Oregon Coast Range and other steep environments [see Table 1 in *Stock and Dietrich*, 2003]. Alternate bar and plane bed streams are also observed to occupy a similar range of slopes in the field (though plane beds are observed up to slopes >0.1), which was initially observed by *Montgomery et al*. [1995], but are only predicted to overlap in a narrow range of slopes (0.009 and 0.06). This suggests that while a large width-to-depth ratio (>12) appears to be important for the development of alternate bars, there are other factors or processes that must ultimately control whether alternate bars or a plane bed state will emerge. The predominance of one channel state over the other could be due to differences in confinement, sediment supply, grain size distributions, or nearby perturbations (e.g., a bridge or road, large woody debris, or an upstream meander bend) [*Lisle et al*., 1991; *Montgomery et al*., 1995; *Livers and Wohl*, 2015].

Regression modeling that assumes that bed slope, grain size, and channel width are independent variables will overemphasize the importance of slope. This approach does not explicitly state the physical mechanisms underlying channel form and bed form formation. In addition, the correlation we find between controlling variables and slope may not hold for all settings. For example, in laboratory flumes or with the introduction of different materials to a river system (e.g., ravel following a fire or woody debris), our predictions of the stable channel configuration may be incorrect. Flume experiments by *Lisle et al*. [1991] and *Weichert et al*. [2008] resulted in the development of alternate bars at slopes between ~0.03 and ~0.1, which is within the bed slope range predicted by theory (Figure 3a), but outside of the range where alternate bars are typically observed in nature. *Weichert et al*. [2008] attribute the stability of alternate bars over step-pools in these experiments to high jamming ratios ($B/D_{84} > 15$), where granular chains did not extend the entire channel width. Designing experiments or artificial channels to have a specific channel morphology may also be problematic, especially if plane bed conditions are desired. There are no simple criteria that distinguish plane bed data from other channel types, aside from having a median bed slope between that for alternate bar and step-pool channels (Figure S1). The slope distribution of all three channel types overlap, however, such that it is just as likely bars or steps will develop as a plane bed.

There has been much debate as to whether step-pools are the result of keystone deposition under supercritical flow conditions [e.g., *Grant et al*., 1990] or the development of a jammed state in streambed sediments [*Church and Zimmermann*, 2007]. While the mechanism cannot be identified from our data set, we do predict that step-pools that form under high Froude conditions would likely occur at lower slopes (< 0.06) than jamming-dominated step-pools (> 0.06) (Figures 3a and 3d). This is close to the transition slope noted by *Church and Zimmermann* [2007], who determined that below slopes of ~0.07, step-pools appear to develop under high transport rates in a manner consistent with antidunes, whereas for gradients greater than 0.07, clasts are jammed and remain anchored, creating stable steps. It is possible that part of the reason we see a mix of step-pool, plane bed, and alternate bar streams between $0.009 < S < 0.06$ is due to changes in channel states over flood timescales [e.g., *Turowski et al*., 2009]. In contrast, channel forms may be more persistent in steeper rivers because of jamming [*Church and Zimmermann*, 2007] or infrequent large magnitude discharges capable of removing steps [*Kondolf et al*., 1991].

We proposed that a controlling variable for the onset of cascade morphology is the ratio of the bankfull Shields stress to the critical Shields stress for debris flow initiation, with the expectation that we would

observe cascade stream morphologies when the ratio nears unity if cascade channels are related to in-channel debris flow initiation. The field data show that none of the stream types have ratios close to one, but cascade streams do have the highest observed ratios, with a median of 0.5, while alternate bar, plane bed, and step-pool streams have median ratios closer to 0.1. The fact that cascade streams have $\tau^*_{bf}/\tau^*_{c,df}$ less than unity could be because cascade morphologies are not related to debris flows, debris flows initiate from landslides, not by in-channel bed failure, or that cascade morphology marks the downstream extent of debris flow transport and deposition, rather than initiation.

Interestingly, while the empirical predictions for bankfull width, depth, and slope (equations (8)–(10)) are functions of gravity ($H \sim g^{-0.2}$, $B \sim g^{-0.2}$, $S \sim g^{0.17}$), which can have implications for hydraulic reconstructions on other planetary surfaces, such as Mars, the derived expressions for the Froude number, width-to-depth ratio, jamming ratio, and the ratio of the bankfull Shields stress to the critical Shields stress for in-channel debris flow initiation are all independent of gravity. However, all of our relations, with the exception of the width-to-depth ratio, are functions of submerged specific density (R). This implies different bed morphologies for a given channel slope on, for example, Titan, where R might range from 1.2 to 2.3 [*Burr et al*., 2006].

In conclusion, we synthesized relationships that highlight the bed slope dependence of hydraulic and geometric variables hypothesized to control channel state in mountain streams. In doing so, we found that the controlling variables correlate with bed slope such that certain bed slopes should correspond to unique channel states, whereas others correspond to multiple channel states. The fact that multiple channel morphologies are predicted and observed within certain bed slope regimes points to a competition of underlying processes where the "winner" is likely dictated by local conditions. Recognizing that channel type cannot simply be correlated with bed slope is important when predicting channel (and hydraulic) conditions in unique environments, especially in places impacted by human or natural disturbances (e.g., postfire stream networks), in artificial streams or flumes, or other planetary surfaces.

Acknowledgments
Funding was provided to M.P.L. by a National Science Foundation grant (EAR-1349115) and to M.C.P. by a National Science Foundation Postdoctoral Fellowship (EAR-1452337). We thank Eric Kleinsasser for his work on compiling step-pool data. This work also benefited from insightful comments from two anonymous reviewers. Stream data compiled and used in this work are available in the supporting information.

References

Aberle, J., and G. M. Smart (2003), The influence of roughness structure on flow resistance on steep slopes, *J. Hydraul. Res.*, *41*(3), 259–269, doi:10.1080/00221680309499971.

Abrahams, A. D., G. Li, and J. F. Atkinson (1995), Step-pool streams: Adjustment to maximum flow resistance, *Water Resour. Res.*, *31*, 2593–2602, doi:10.1029/95WR01957.

Altunkaynak, A., and K. B. Strom (2009), A predictive model for reach morphology classification in mountain streams using multilayer perceptron methods, *Water Resour. Res.*, *45*, W12501, doi:10.1029/2009WR008055.

Bathurst, J., H. Cao, and W. Graf (1984), Hydraulics and sediment transport in a steep flume: Data from the EPFL study, pp. 1–57, Rep. Cent. Ecol. Hydrol. Wallingford U. K.

Brayshaw, A. C., L. E. Frostick, and I. Reid (1983), The hydrodynamics of particle clusters and sediment entrapment in coarse alluvial channels, *Sedimentology*, *30*(1), 137–143, doi:10.1111/j.1365-3091.1983.tb00656.x.

Buffington, J. M., and D. R. Montgomery (1999), Effects of hydraulic roughness on surface textures of gravel-bed rivers, *Water Resour. Res.*, *35*(11), 3507–3521.

Buffington, J. M., and D. R. Montgomery (2013), Geomorphic classification of rivers, in *Treatise on Geomorphology*, vol. 9, edited by J. Shroder and E. Wohl, pp. 730–767, Fluvial Geomorphol., Academic Press, San Diego, Calif.

Burr, D. M., J. P. Emery, R. D. Lorenz, G. C. Collins, and P. A. Carling (2006), Sediment transport by liquid surficial flow: Application to Titan, *Icarus*, *181*(1), 235–242.

Chin, A. (1989), Step pools in stream channels, *Prog. Phys. Geogr.*, *13*(3), 391–407, doi:10.1177/030913338901300304.

Chin, A. (1999), On the origin of step-pool sequences in mountain streams, *Geophys. Res. Lett.*, *26*, 231–234, doi:10.1029/1998GL900270.

Church, M. (2002), Geomorphic thresholds in riverine landscapes, *Freshw. Biol.*, *47*(4), 541–557, doi:10.1046/j.1365-2427.2002.00919.x.

Church, M., and D. McLean (1994), Sedimentation in lower Fraser River, British Columbia: Implications for management, Var. Large Alluv. Rivers, 221–241.

Church, M., and K. Rood (1983), *Catalog of Alluvial River Channel Regime Data*, 99 pp., Vancouver, Dep. of Geogr., Univ. of British Columbia.

Church, M., and A. Zimmermann (2007), Form and stability of step-pool channels: Research progress, *Water Resour. Res.*, *43*, W03415, doi:10.1029/2006WR005037.

Colombini, M., G. Seminara, and M. Tubino (1987), Finite-amplitude alternate bars, *J. Fluid Mech.*, *181*, 213–232, doi:10.1017/S0022112087002064.

Cui, Y., and G. Parker (2005), Numerical model of sediment pulses and sediment-supply disturbances in mountain rivers, *J. Hydraul. Eng.*, *131*(8), 646–656.

DiBiase, R. A., A. M. Heimsath, and K. X. Whipple (2012), Hillslope response to tectonic forcing in threshold landscapes, *Earth Surf. Process. Landf.*, *37*(8), 855–865, doi:10.1002/esp.3205.

Dietrich, W. E., and J. D. Smith (1983), Influence of the point bar on flow through curved channels, *Water Resour. Res.*, *19*, 1173–1192, doi:10.1029/WR019i005p01173.

Dietrich, W. E., and P. Whiting (1989), Boundary shear stress and sediment transport in river meanders of sand and gravel, in *River Meandering*, edited by S. Ikeda and G. Parker, pp. 1–50, AGU, Washington, D. C.

Engelund, F., and J. Fredsoe (1982), Sediment ripples and dunes, *Annu. Rev. Fluid Mech.*, *14*(1), 13–37.

Ferguson, R. (2007), Flow resistance equations for gravel- and boulder-bed streams, *Water Resour. Res.*, *43*, W05427, doi:10.1029/2006WR005422.
Flores, A. N., B. P. Bledsoe, C. O. Cuhaciyan, and E. E. Wohl (2006), Channel-reach morphology dependence on energy, scale, and hydroclimatic processes with implications for prediction using geospatial data, *Water Resour. Res.*, *42*, W06412, doi:10.1029/2005WR004226.
Garcia, M. H. (2008), Sediment transport and morphodynamics, Sediment. Eng. Process. Meas. Model. Pract., (110).
Grant, G. E., and T. Mizuyama (1991), Origin of step-pool sequences in high gradient streams: A flume experiment, in *Proceedings of the Japan–US Workshop on Snow Avalanche: Landslide, Debris Flow Prediction and Control: Tsukuba, Japan, Organizing Committee of the Japan–US Workshop on Snow Avalanche, Landslide, Debris Flow Prediction and Control*, pp. 523–532, Sci. and Technol. Agency of Jpn. Gov., Tsukuba, Japan.
Grant, G. E., F. J. Swanson, and M. G. Wolman (1990), Pattern and origin of stepped-bed morphology in high-gradient streams, western cascades, Oregon, *Geol. Soc. Am. Bull.*, *102*(3), 340–352, doi:10.1130/0016-7606(1990)102<0340:PAOOSB>2.3.CO;2.
Hassan, M. A., and I. Reid (1990), The influence of microform bed roughness elements on flow and sediment transport in gravel bed rivers, *Earth Surf. Process. Landf.*, *15*(8), 739–750, doi:10.1002/esp.3290150807.
Hendershot, M. L., J. G. Venditti, R. W. Bradley, R. A. Kostaschuk, M. Church, and M. A. Allison (2016), Response of low-angle dunes to variable flow, *Sedimentology*, *63*(3), 743–760, doi:10.1111/sed.12236.
Johnson, J. P. L., and K. X. Whipple (2010), Evaluating the controls of shear stress, sediment supply, alluvial cover, and channel morphology on experimental bedrock incision rate, *J. Geophys. Res.*, *115*, F02018, doi:10.1029/2009JF001335.
Judd, H. E. (1963), *A Study of Bed Characteristics in Relation to Flow in Rough, High-Gradient, Natural Channels*, PhD thesis, 115 pp., Utah State Univ, Logan.
Kennedy, J. F. (1963), The mechanics of dunes and antidunes in erodible-bed channels, *J. Fluid Mech.*, *16*(4), 521–544, doi:10.1017/S0022112063000975.
Kondolf, G. M., G. F. Cada, M. J. Sale, and T. Felando (1991), Distribution and stability of potential salmonid spawning gravels in steep boulder-bed streams of the eastern Sierra Nevada, *Trans. Am. Fish. Soc.*, *120*(2), 177–186, doi:10.1577/1548-8659(1991)120<0177:DASOPS>2.3.CO;2.
Lamb, M. P., W. E. Dietrich, and J. G. Venditti (2008), Is the critical Shields stress for incipient sediment motion dependent on channel-bed slope?, *J. Geophys. Res.*, *113*, F02008, doi:10.1029/2007JF000831.
Lamb, M. P., J. P. Grotzinger, J. B. Southard, and N. J. Tosca (2012), Were aqueous ripples on Mars formed by flowing brines, *Sediment. Geol. Mars*, *102*, 139–150.
Lamb, M. P., F. Brun, and B. M. Fuller (2017), Hydrodynamics of steep streams with planar coarse-grained beds: Turbulence, flow resistance, and implications for sediment transport, *Water Resour. Res.*, *53*, 2240–2263, doi:10.1002/2016WR019579.
Li, C., M. J. Czapiga, E. C. Eke, E. Viparelli, and G. Parker (2015), Variable Shields number model for river bankfull geometry: Bankfull shear velocity is viscosity-dependent but grain size-independent, *J. Hydraul. Res.*, *53*(1), 36–48, doi:10.1080/00221686.2014.939113.
Lisle, T. E., H. Ikeda, and F. Iseya (1991), Formation of stationary alternate bars in a steep channel with mixed-size sediment: A flume experiment, *Earth Surf. Process. Landf.*, *16*(5), 463–469, doi:10.1002/esp.3290160507.
Livers, B., and E. Wohl (2015), An evaluation of stream characteristics in glacial versus fluvial process domains in the Colorado Front Range, *Geomorphology*, *231*, 72–82, doi:10.1016/j.geomorph.2014.12.003.
Milliman, J. D., and J. P. M. Syvitski (1992), Geomorphic/tectonic control of sediment discharge to the ocean: The importance of small mountainous rivers, *J. Geol.*, *100*(5), 525–544.
Montgomery, D. R., and J. M. Buffington (1997), Channel-reach morphology in mountain drainage basins, *Geol. Soc. Am. Bull.*, *109*(5), 596–611, doi:10.1130/0016-7606(1997)109<0596:CRMIMD>2.3.CO;2.
Montgomery, D. R., J. M. Buffington, R. D. Smith, K. M. Schmidt, and G. Pess (1995), Pool Spacing in Forest Channels, *Water Resour. Res.*, *31*(4), 1097–1105.
Montgomery, D. R., T. M. Massong, and S. C. S. Hawley (2003), Influence of debris flows and log jams on the location of pools and alluvial channel reaches, Oregon coast range, *Geol. Soc. Am. Bull.*, *115*(1), 78–88, doi:10.1130/0016-7606(2003)115<0078:IODFAL>2.0.CO;2.
Nelson, P. A., W. E. Dietrich, and J. G. Venditti (2010), Bed topography and the development of forced bed surface patches, *J. Geophys. Res.*, *115*, F04024, doi:10.1029/2010JF001747.
Nitsche, M., D. Rickenmann, J. M. Turowski, A. Badoux, and J. W. Kirchner (2011), Evaluation of bedload transport predictions using flow resistance equations to account for macro-roughness in steep mountain streams, *Water Resour. Res.*, *47*, W08513, doi:10.1029/2011WR010645.
O'Neill, M. P., and A. D. Abrahams (1984), Objective identification of pools and riffles, *Water Resour. Res.*, *20*, 921–926, doi:10.1029/WR020i007p00921.
Paola, C., P. L. Heller, and C. L. Angevine (1992), The large-scale dynamics of grain-size variation in alluvial basins, 1: Theory, *Basin Res.*, *4*(2), 73–90.
Parker, G. (1978), Self-formed straight rivers with equilibrium banks and mobile bed. Part 2. The gravel river, *J. Fluid Mech.*, *89*(1), 127–146, doi:10.1017/S0022112078002505.
Parker, G. (2004), 1D sediment transport morphodynamics with applications to rivers and turbidity currents, E-book, St. Anthony Falls Lab Univ Minn Minneap. Httphydrolab Ill. Edupeopleparkergmorphodynamicse-Book Htm.
Parker, G., and N. Izumi (2000), Purely erosional cyclic and solitary steps created by flow over a cohesive bed, *J. Fluid Mech.*, *419*, 203–238.
Parker, G., C. Paola, K. X. Whipple, and D. Mohrig (1998), Alluvial fans formed by channelized fluvial and sheet flow. I: Theory, *J. Hydraul. Eng.*, *124*(10), 985–995.
Parker, G., P. R. Wilcock, C. Paola, W. E. Dietrich, and J. Pitlick (2007), Physical basis for quasi-universal relations describing bankfull hydraulic geometry of single-thread gravel bed rivers, *J. Geophys. Res.*, *112*, F04005, doi:10.1029/2006JF000549.
Pfeiffer, A. M., N. J. Finnegan, and J. K. Willenbring (2017), Sediment supply controls equilibrium channel geometry in gravel rivers, *Proc. Natl. Acad. Sci.*, *114*(13), 3346–3351.
Prancevic, J. P., M. P. Lamb, and B. M. Fuller (2014), Incipient sediment motion across the river to debris-flow transition, *Geology*, *42*(3), 191–194, doi:10.1130/G34927.1.
Rickenmann, D., and A. Recking (2011), Evaluation of flow resistance in gravel-bed rivers through a large field data set, *Water Resour. Res.*, *47*, W07538, doi:10.1029/2010WR009793.
Rosgen, D. L. (1994), A classification of natural rivers, *Catena*, *22*(3), 169–199.
Rosgen, D. L. (1996), *Applied River Morphology*, 350 pp., Wildland Hydrology, Pagosa Springs, Colo.
Rubin, D., and D. McCulloch (1980), Single and superimposed bedforms: A synthesis of San Francisco Bay and flume observations, *Sediment. Geol.*, *26*(1–3), 207–231.

Selby, M. J. (1993), *Hillslope Materials and Processes*, 451 pp., Oxford Univ. Press, New York.
Shreve, R. L. (1969), Stream lengths and basin areas in topologically random channel networks, *J. Geol.*, *77*(4), 397–414.
Southard, J. (1991), Experimental determination of bed-form stability, *Annu. Rev. Earth Planet. Sci.*, *19*(1), 423–455, doi:10.1146/annurev.ea.19.050191.002231.
Southard, J. B., and L. A. Boguchwal (1990), Bed configurations in steady unidirectional water flows. Part 2. Synthesis of flume data, *J. Sediment. Res.*, *60*(5), doi:10.1306/212F9241-2B24-11D7-8648000102C1865D.
Stock, J., and W. E. Dietrich (2003), Valley incision by debris flows: Evidence of a topographic signature, *Water Resour. Res.*, *39*(4), 1089, doi:10.1029/2001WR001057.
Takahashi, T. (1978), Mechanical characteristics of debris flow, *J. Hydraul. Div.*, *104*(8), 1153–1169.
Taki, K., and G. Parker (2005), Transportational cyclic steps created by flow over an erodible bed. Part 1. Experiments, *J. Hydraul. Res.*, *43*(5), 488–501.
Trampush, S. M., S. Huzurbazar, and B. McElroy (2014), Empirical assessment of theory for bankfull characteristics of alluvial channels, *Water Resour. Res.*, *50*, 9211–9220, doi:10.1002/2014WR015597.
Turowski, J. M., E. M. Yager, A. Badoux, D. Rickenmann, and P. Molnar (2009), The impact of exceptional events on erosion, bedload transport and channel stability in a step-pool channel, *Earth Surf. Process. Landf.*, *34*(12), 1661–1673.
Vanoni, V. A., and L.-S. Hwang (1967), Bed forms and friction in streams, *J. Hydraul. Div.*, *93*, 121–144.
Venditti, J. G. (2007), Turbulent flow and drag over fixed two- and three-dimensional dunes, *J. Geophys. Res.*, *112*, F04008, doi:10.1029/2006JF000650.
Weichert, R. B., G. R. Bezzola, and H.-E. Minor (2008), Bed morphology and generation of step–pool channels, *Earth Surf. Process. Landf.*, *33*(11), 1678–1692.
Whittaker, J. G., and M. N. R. Jaeggi (1982), Origin of step-pool systems in mountain streams, *J. Hydraul. Div.*, *108*(6), 758–773.
Wohl, E., and D. Merritt (2005), Prediction of mountain stream morphology, *Water Resour. Res.*, *41*, W08419, doi:10.1029/2004WR003779.
Wohl, E., and D. M. Merritt (2008), Reach-scale channel geometry of mountain streams, *Geomorphology*, *93*(3–4), 168–185, doi:10.1016/j.geomorph.2007.02.014.
Yager, E. M., J. M. Turowski, D. Rickenmann, and B. W. McArdell (2012), Sediment supply, grain protrusion, and bedload transport in mountain streams, *Geophys. Res. Lett.*, *39*, L10402, doi:10.1029/2012GL051654.
Zimmermann, A. (2010), Flow resistance in steep streams: An experimental study, *Water Resour. Res.*, *46*, W09536, doi:10.1029/2009WR007913.
Zimmermann, A., and M. Church (2001), Channel morphology, gradient profiles and bed stresses during flood in a step–pool channel, *Geomorphology*, *40*(3–4), 311–327, doi:10.1016/S0169-555X(01)00057-5.
Zimmermann, A., M. Church, and M. A. Hassan (2010), Step-pool stability: Testing the jammed state hypothesis, *J. Geophys. Res.*, *115*, F02008, doi:10.1029/2009JF001365.